Experimental study of thermoelectricity in superconducting indium

D. J. Van Harlingen,* D. F. Heidel, and J. C. Garland
Department of Physics, Ohio State University, Columbus, Ohio 43210
(Received 23 August 1979)

This paper reports on a comprehensive study of thermoelectricity in pure superconducting indium near the transition temperature. The samples consisted of hollow bimetallic toroids of lead and indium. Upon application of a temperature gradient, a magnetic flux was produced within the hollow cavity of the toroids which could be coupled, via a superconducting flux transformer, into a superconducting quantum interference device magnetometer. The thermoelectric origins of the magnetic flux and the experimental method are discussed in detail. The magnetic flux was measured in seven specimens, and in each was found to diverge as the transition temperature was approached with a $(1-T/T_c)^{-3/2}$ power-law dependence. The magnitude of the flux varied by about a factor of 40 among the different samples and appeared to scale with the normal-state thermoelectric properties of the indium. Tests intended to eliminate possible spurious causes for the magnetic flux are also discussed.

I. INTRODUCTION

It is well known that most of the equilibrium properties of the superconducting state can be explained by the microscopic BCS theory and by the phenomenological Ginzburg-Landau theory. Within the past few years, however, interest has focused on the nonequilibrium properties of superconductors, where the theoretical framework is less well understood. Eliashberg,[1] Schmid and Schön,[2] and Pethick and Smith[3] have derived kinetic equations which characterize the quasiparticle distribution function of superconductors, while several other authors[4–6] have been concerned specifically with quasiparticle scattering and recombination.

In contrast to studies of normal metals, most experimental studies of the nonequilibrium state of superconductors have involved tunneling measurements. In normal metals, such studies are usually made through measurements of transport properties—the electrical resistivity, thermal conductivity, and various thermoelectric coefficients. Most of these transport coefficients vanish in the superconducting state, including all conventional thermoelectric coefficients such as the thermoelectric power, the Seebeck coefficient, and the Thomson and Peltier heats. A useful review of thermoelectricity in superconductors may be found in the recent article by Matsinger *et al.*[7]

In this paper, we wish to consider a thermoelectric transport effect which exists only in the superconducting state. Measurements of this effect, whose existence was proposed in 1974 by Garland and Van Harlingen[8] and independently by Gal'perin *et al.*,[9] provide a useful means for studying quasiparticle currents in superconductors. The effect is based on an observation by Ginzburg[10] in 1944 that a current of quasiparticles can be driven by a temperature gradient, much as ordinary thermoelectric current is produced in a normal metal. In a superconductor, however, this quasiparticle current is always accompanied by a counterflow of supercurrent. This superconducting counterflow ordinarily cancels the quasiparticle current, although recent work[11,12] suggests that the cancellation is not complete in anisotropic materials. As a consequence of this cancellation, any experiment intended to study thermoelectricity in superconductors must be able to differentiate between the quasiparticle and superfluid components of the currents.

In the experiment reported here, this differentiation is accomplished by measuring a magnetic flux whose origin is a phase gradient of the supercondutting order parameter. As pointed out by Gal'perin, *et al.*,[9] such a phase gradient always accompanies the counterflow of superfluid current resulting from a temperature gradient. In a simply connected superconductor, the phase variation of the order parameter is not observable. However, in a bimetallic ring geometry, the constraint that the total phase length be a multiple of 2π can be satisfied only if a magnetic flux is produced through the center of the ring. As will be shown in Sec. II, this flux can be expressed as

$$\Phi_T=\int_{T_2}^{T_1}[\Omega^a(T)-\Omega^b(T)]dT \quad . \tag{1}$$

In the above expression, $\Omega^a(T)$ and $\Omega^b(T)$ are thermoelectric transport coefficients associated with each of the two superconductors in the ring, while T_1 and T_2 are the temperatures of the junctions connecting the two superconductors. The thermoelectric coefficient $\Omega(T)$ is dependent on the detailed form of the quasiparticle distribution function and also on the value of the superconducting order parameter of the metal. As is evident from Eq. (1), the flux Φ_T is determined by the thermoelectric properties of each superconductor comprising the ring. The flux vanishes either if the ring is in thermal equilibrium, i.e., if $T_1 = T_2$, or if $\Omega^a(T) = \Omega_b(T)$, as would occur if the ring were made of a single metal. As shown in Ref. 8, the thermoelectric flux is predicted to be much smaller than a flux quantum Φ_0, except near T_c where $\Omega(T)$ is expected to diverge logarithmically. Near T_c, Φ_T was estimated by Ref. 8 to be large enough to resolve with a superconducting quantum interference device (SQUID) magnetometer.

The prediction of a measurable thermoelectric flux effect in superconductors has revived a long-standing theoretical interest in the subject. A kinetic theory for the transport coefficient $\Omega(T)$ has been developed by Gal'perin *et al.*,[9] who assumed that the quasiparticles in a superconductor have the same mean-free path as the conduction electrons in a normal metal. Kon[13] has predicted an enhancement of the flux effect in superconductors containing nonmagnetic impurties with localized states near the Fermi energy, while the effect of superfluid flow on thermoelectricity has been examined by Aronov,[14] Kozub,[15] and Heidel and Garland.[16] The interface between two different superconductors comprising a ring has been considered in detail by Artemenko and Volkov,[17] who have predicted a small additional contribution to the flux Φ_T. Very recent theoretical contributions to the subject have also been made by Pethick and Smith,[18] Schmid and Schön,[19] and Sacks.[20]

There have been several recent attempts to verify the existence of the thermoelectric flux effect in superconductors. Zavaritskii[21] first reported observing the effect in a Pb-Sn loop, while subsequent experiments on Nb-Ta loops by Pegrum *et al.*[22] and Falco,[23] also produced measurable results. Each of these experiments yielded a divergent flux at T_c, as expected, although the magnitude of the flux appeared to be much larger than predicted. Recently, Pegrum and Guénault[24] have suggested that all of these observations could actually have been caused by temperature dependent penetration depth changes in the superconductors rather than by the thermoelectric flux effect. They further expressed doubt that the technique used in these experiments would be capable of distinguishing the true thermoelectric flux from other spurious sources of flux.

In this paper, we report the results of a study of the thermoelectric flux effect in superconducting In-Pb samples, using a different technique from earlier studies. A preliminary account of our work appears in Ref. 25. Our technique is based on the use of a toroidal sample geometry which makes possible a substantial improvement in resolution and in immunity to spurious effects over the configuration used in other experiments. The flux measured in our experiment, which we believe to arise from a thermoelectric mechansim, is several orders of magnitude larger than that suggested by Ref. 8 and has a more rapid divergence than predicted. In Sec. II of this paper, we discuss the basic mechanism of the thermoelectric flux effect, deriving expressions for the flux Φ_T and for the thermoelectric coefficient $\Omega(T)$. Section III contains a description of the magnetometer technique used to measure the thermoelectric flux. In Sec. IV we report our measurements of the thermoelectric flux in superconducting In-Pb samples. A discussion of these measurements is in Sec. V.

II. THEORY

A. Basic concepts

In a normal metal, an electric current is driven by an electric field and a temperature gradient according to the transport equation

$$\vec{J} = \sigma\vec{E}' + L_T(-\vec{\nabla}T) \quad . \tag{2}$$

In the first term, an expression of Ohm's law, σ is the electrical conductivity and $\vec{E}'$ is the electrical driving force

$$\vec{E}' = \vec{E} - \frac{1}{e}\vec{\nabla}\mu \tag{3}$$

containing, in addition to the true electric field $\vec{E}$, a term in the chemical potential μ. For steady-state fields, we can write $\vec{E}' = -(1/e)\vec{\nabla}\phi$, where ϕ is the electrochemical potential defined by

$$\phi = eV + \mu \quad , \tag{4}$$

with V the electrostatic potential; a conventional voltmeter measures differences of the electrochemical potential. In general, $\vec{E}'$ must also contain a term $-(1/c)\dot{\vec{A}}$ for gauge invariance.

The second term in Eq. (2) is the thermoelectric contribution to the current characterized by the transport coefficient L_T. L_T is ordinarily measured in conjunction with other transport coefficients. For example, as shown in Fig. 1(a), an electric field can be established in an isolated metal sample to null out the thermally induced diffusion current. Measuring the ratio of $\vec{E}'$ to $\vec{\nabla}T$ in this configuration yields the familiar thermoelectric power $S = L_T/\sigma$, from which L_T can be obtained.

In pure type-I superconductor, the picture is complicated by the presence of the superfluid condensate, whose electrodynamical properties are described by the London equations:

$$\vec{\nabla} \times (\Lambda\vec{J}_s) = -\frac{1}{c}\vec{B} \quad , \tag{5}$$

$$\frac{\partial}{\partial t}(\Lambda\vec{J}_s) = \vec{E}' = -\frac{1}{e}\vec{\nabla}\phi - \frac{1}{c}\dot{\vec{A}} \quad . \tag{6}$$

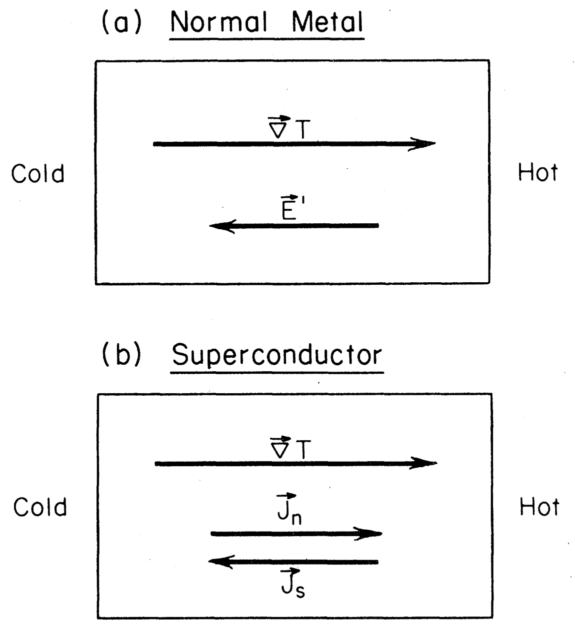

FIG. 1. (a) In an open-circuited normal metal, a temperature gradient $\vec{\nabla} T$ induces an electric field $\vec{E}'$. (b) In an open-circuited superconductor, a temperature gradient $\vec{\nabla} T$ drives a quasiparticle current $\vec{J}_n$ which is locally canceled by a counterflow of supercurrent $\vec{J}_s$.

Here $\vec{J}_s$ is the superfluid current density and Λ is the London parameter, given by $\Lambda = m/(e^2 n_s)$, where n_s is the density of superconducting electrons. The electrical driving force $\vec{E}'$ and the electrochemical potential ϕ are defined by Eqs. (3) and (4), where it should be understood that the chemical potential is that of the superfluid condensate, i.e., $\mu = \mu_s$. In the steady state, $\vec{E}' = -(1/e)\vec{\nabla}\phi = 0$; note, however, that this condition does not mean that the electric field also vanishes. From Eq (3), we see that in the presence of a temperature gradient there exists an electric field $\vec{E} = (1/e)\vec{\nabla}\mu_s$ in the superconductor, which can be measured using an electrostatic voltmeter.[26] Electric fields are also produced in the vicinity of an interface between a superconductor and a dielectric, normal metal, or another superconductor.[27,28]

Thermoelectric currents in superconductors are carried by quasiparticle excitations. Despite their inherent many-body nature, these excitations respond to external fields in much the same way as the conduction electrons in a normal metal and are governed by a transport equation analogous to Eq. (2):

$$\vec{J}_n = \sigma \vec{E}_n' + L_T(-\vec{\nabla} T) \ . \tag{7}$$

In the above expression $\vec{E}_n'$ refers to the electrical driving force of the quasiparticles. This force may be written as $\vec{E}_n' = \vec{E} - (1/e)\vec{\nabla}\mu_n$, where μ_n is the chemcial potential of the quasiparticle excitations, which may differ from the superfluid chemical potential μ_s. Since $\vec{E} = (1/e)\vec{\nabla}\mu_s$, Eq. (7) may be expressed as

$$\vec{J}_n = \frac{\sigma}{e}\vec{\nabla}(\mu_s - \mu_n) + L_T(-\vec{\nabla} T) \ . \tag{7a}$$

From this equation we see that the difference between the superfluid and normal fluid chemical potentials may be regarded as the effective electrical driving force for the quasiparticles. As shown recently by Pethick and Smith,[3] such a difference can exist in regions where normal current is converted into supercurrent. In our experiment, such a region occurs at the ends of the sample where there is a heat flow into the superconductor. There the potential difference $(\mu_s - \mu_n)$ decays exponentially into the superconductor over a quasiparticle diffusion length and is zero in the rest of the sample. Thus, except in this region, the normal current is given simply by

$$\vec{J}_n = -L_T \vec{\nabla} T \ . \tag{7b}$$

Note that the thermoelectric transport coefficient L_T may be quite different from its equivalent normal-state value. There is, in fact, no reason why L_T should even be continuous across the superconducting transition.

In thermal equilibrium, $\vec{J}_n = 0$, so that Eq. (5) may be combined with Maxwell's equation to yield

$$\nabla^2 \vec{B} = (1/\lambda)^2 \vec{B} \ , \tag{8}$$

where λ is the London penetration depth given by $(c^2\Lambda/4\pi)^{1/2}$. Equation (8) reflects the Meissner effect, the exclusion of magnetic field from the bulk of a superconductor. In an isotropic, homogeneous superconductor, $\vec{\nabla} \times \vec{J}_n = 0$ even out of thermal equilibrium, so that Eq. (8) is still valid; in other words, the field profile is unchanged by the presence of the quasiparticle current $\vec{J}_n$. Thus $\vec{J}_n$ is canceled locally throughout the superconductor by a counterflow of supercurrent, as illustrated in Fig. 1(b). Any net current consists of excess supercurrents flowing on the surface (within the penetration depth) in response to externally applied magnetic fields. In the interior of the superconductor, $\vec{B} = 0$, so that the total supercurrent is given by

$$\vec{J}_s = -\vec{J}_n = L_T \vec{\nabla} T \ . \tag{9}$$

It is the cancellation of the thermoelectric current $\vec{J}_n$ as well as the absence of any electrochemical potential difference in bulk superconductors which have led to the general belief that thermoelectric effects do not exist in superconductors.

B. Thermoelectric flux

The basis for the thermoelectric flux effect is the long-range phase coherence of the superconducting condensate. The condensate can be described by a complex order parameter $\psi_s(\vec{r})$, which can be written as

$$\psi_s(\vec{r}) = (n_s/2)^{1/2} e^{i\theta(\vec{r})} \quad . \tag{10}$$

In terms of ψ_s, the supercurrent $\vec{J}_s$ is given by

$$\vec{J}_s = 2e\left[\frac{\hbar}{4mi}(\psi_s^* \vec{\nabla}\psi_s - \psi_s \vec{\nabla}\psi_s^*) - \frac{e}{mc}\vec{A}\psi_s^*\psi_s\right] \quad . \tag{11}$$

Combining Eqs. (10) and (11) yields an expression for the phase of the order parameter:

$$\vec{\nabla}\theta = \frac{2m}{e\hbar n_s}\vec{J}_s + \frac{2e}{\hbar c}\vec{A} = \frac{2m}{e\hbar}\frac{L_T}{n_s}\vec{\nabla}T + \frac{2e}{\hbar c}\vec{A} \quad . \tag{12}$$

Choosing the gauge for which $\vec{A}=0$, we obtain a phase difference between the ends of the superconductor of Fig. 1(b) given by

$$\Delta\theta = \left[\frac{2m}{e\hbar}\frac{L_T}{n_s}\right]\Delta T \quad . \tag{13}$$

The phase difference $\Delta\theta$ cannot be measured directly in a sample like that of Fig. 1(b); we can deduce $\Delta\theta$ indirectly, however, by forming a thermocouple out of two superconductors.

Let us first consider a thermocouple consisting of normal metals. In a normal metal, we can write Eq. (2) in terms of the electrochemical potential ϕ to obtain the expressions

$$\vec{\nabla}\phi = -eS\vec{\nabla}T - \frac{e}{\sigma}\vec{J} \quad , \tag{14}$$

which is the normal-state analog of Eq. (12), and

$$\Delta\phi = eS\Delta T \quad , \tag{15}$$

which is analogous to Eq. (13) (if the normal metal is open circuited). If we form an open-circuited thermocouple of two dissimilar normal metals, as in Fig. 2(a), the difference in electrochemical potential across the ends of the thermocouple is given by

$$\Delta\phi = e(S^a - S_b)\Delta T \quad , \tag{16}$$

where S^a and S^b are the thermoelectric powers of the two metals in the thermocouple. Closing the loop, by connecting the ends of the thermocouple together, then yields

$$\oint \vec{\nabla}\phi \cdot d\vec{l} = 0 \quad , \tag{17}$$

which by Eq. (16) requires a circulating thermoelectric current $\vec{J}$ in the loop.

An analogous effect occurs for the superconducting thermocouple of Fig. 2(b). When open circuited, there is a phase difference across the ends of the thermocouple that depends on the properties of each

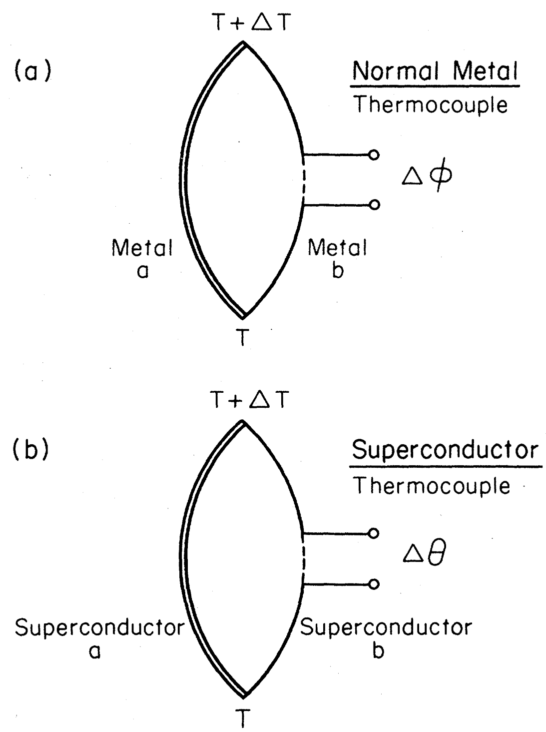

FIG. 2. (a) An electrochemical potential difference $\Delta\phi$ appears across an open-circuited thermocouple composed of two normal metals. A circulating thermoelectric current flows around the loop if the two ends of the thermocouple are connected together. (b) A quantum-mechanical phase difference $\Delta\theta$ appears across an open-circuited thermocouple composed of two superconducting metals. A circulating supercurrent flows around the loop if the two ends of the thermocouple are connected together.

metal; i.e.,

$$\Delta\theta = \frac{2m}{e\hbar}\left[\frac{L_T^a}{n_s^a} - \frac{L_T^b}{n_s^b}\right]\Delta T \quad . \tag{18}$$

When the loop is closed as in Fig. 3, the constraint that the order parameter be single valued imposes a restriction on the phase analogous to Eq. (17):

$$\oint \vec{\nabla}\theta \cdot d\vec{l} = 2\pi n \quad . \tag{19}$$

This constraint on the phase can only be satisfied if the total magnetic flux through the closed loop has magnitude

$$\Phi = n\Phi_0 + \Phi_T \quad , \tag{20}$$

where Φ_T is given by

$$\Phi_T = \int_{T_1}^{T_2} \frac{mc}{e^2}\left[\frac{L_T^a}{n_s^a} - \frac{L_T^b}{n_s^b}\right] dT$$

$$= \int_{T_1}^{T_2} [\Omega^a(T) - \Omega^b(T)]\, dT \quad . \tag{21}$$

This result is obtained by integrating Eq. (12) around the bimetallic thermocouple along a path lying in the interior of the superconductors. Note that the coefficients $\Omega^a(T)$ and $\Omega^b(T)$ depend on the thermoelectric coefficient L_T and the superfluid denstiy n_s of their respective superconductor. Ordinarily it is possible to neglect the contribution to the integral in Eq. (21) from the superconductor having the higher transition temperature; if $T_{cb} > T_{ca}$, then $\Omega^b(T) << \Omega^a(T)$. Note also that there is an additional contribution to the flux from the interface regions where normal current is converted to supercurrent. This extra term is of little experimental consequence, however, having been shown by Artemenko and Volkov[17] to be smaller than Φ_T by a factor l/R, where l is the quasiparticle diffusion length and R is the loop radius.

If $\vec{\nabla} T = 0$ or if the loop is homogeneous [so that the expression in parenthesis in Eq. (21) is zero], then Φ_T vanishes and Eq. (20) expresses the familiar quantization of flux in a closed superconducting ring. In general, however, an unquantized flux Φ_T is generated through a bimetallic loop whenever a temperature gradient is present. Like the quantized trapped flux $n\Phi_0$, this thermoelectic flux is produced by supercurrents that flow within the penetration depth on the inside surfaces of the loop.

An interesting aspect of this effect is that it provides a counterexample of the classical idea that the magnetic flux cannot change within a closed ring whose conductivity is infinite. Actually, Maxwell's equations do not prohibit a flux from changing within a perfectly conducting ring so long as the thickness of the ring is smaller than the London penetration depth $\lambda \equiv (mc^2/4\pi n_s e^2)^{1/2}$; in a thick ring, however, both the currents and magnetic fields are confined to within a thickness λ of the surface and are excluded from the interior of the conductor. The constancy of the flux enclosed by such a ring then follows by integrating the London equation (6) around a path buried deep within the ring.

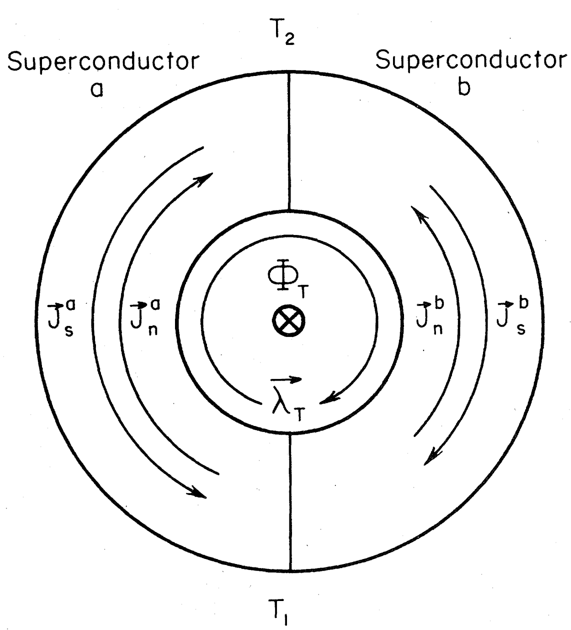

FIG. 3. In a bimetallic superconducting ring whose junctions are maintained at different temperatures, the quasiparticle current $\vec{J}_n$ in each superconductor is locally canceled by a superfluid counterflow $\vec{J}_s$. Phase coherence requires the generation of a magnetic flux produced by circulating surface supercurrents.

In the thermoelectric flux effect, however, this argument breaks down because the superfluid current $\vec{J}_s$ does not vanish inside the conductor; instead it is given by $\vec{J}_s = -\vec{J}_n = L_T \vec{\nabla} T$. The origin of the flux resulting from these thermoelectric currents can then be described qualitatively as follows (we assume for simplicity that initially $\vec{\nabla} T = 0$ and that all currents and fields are zero). Upon the first application of a temperature gradient, a normal current is generated in accordance with the transport equation (7). The magnetic field associated with this current induces an electric field $\vec{E}' = (-1/c)\partial\vec{A}/\partial t$ which begins to accelerate the superfluid, in accordance with the London equation (6). Deep within the superconductor, the superfluid current $\vec{J}_s$ cancels exactly the normal current $\vec{J}_n$, but within the penetration depth this cancellation is not exact. It is this residual current imbalance at the surface which leads to a flux through the ring. Once the temperature gradient has stabilized, the electric field vanishes and the superfluid current stops accelerating. So long as the temperature gradient remains stable, $\vec{J}_s$ remains constant with a value determined by the magnitude of the vector potential. The exact position dependence of $\vec{J}_s$ near the surface could be obtained by solving the classical boundary-value problem for the vector potential, although we have not attempted this solution.

III. EXPERIMENTAL DETAILS

A. Experimental method

As shown in the previous section, a temperature gradient applied to a loop formed from two different superconducting metals will induce a magnetic flux through the loop. Experimentally, this flux may be detected in two different ways: by measuring the flux directly, or by measuring the supercurrents flowing on the surface of the loop which produce the flux. In the experiment reported here, we have used the former method. The flux produced by thermoelectric supercurrents was coupled into an rf-biased SQUID magnetometer by means of a calibrated flux transformer.

1. Sample geometry

Although the simple loop geometry is the easiest to understand, it is not the most desirable experimental configuration. The simple loop is particularly susceptible to problems which arise from external magnetic fields and from temperature dependent changes of the penetration depth. The nature of these problems has been recently discussed by Pegrum and Guénault.[24] Furthermore, the magnitude of the magnetic flux coupled into a SQUID from a simple loop is small and easily obscured by various sources of flux noise.

In our experiment we have used a toroidal sample configuration. As will be discussed subsequently, the toroidal geometry offers improved sensitivity, greater immunity from extraneous fields, and higher resistance to penetration-depth complications than the loop geometry. The toroidal sample is a topological extension of a double loop. As shown in Fig. 4, a double loop consists of a large ring formed of one superconductor (superconductor a) which is short circuited by a second dissimilar superconductor, (superconductor b). If a temperature difference is applied to the junctions between the two superconductors, then a magnetic flux will be induced in each half of the ring. Although the magnitudes of the flux in each half are equal, the directions are reversed, so that the lines of flux may be viewed as circling the center section of superconductor. A toroidal geometry may

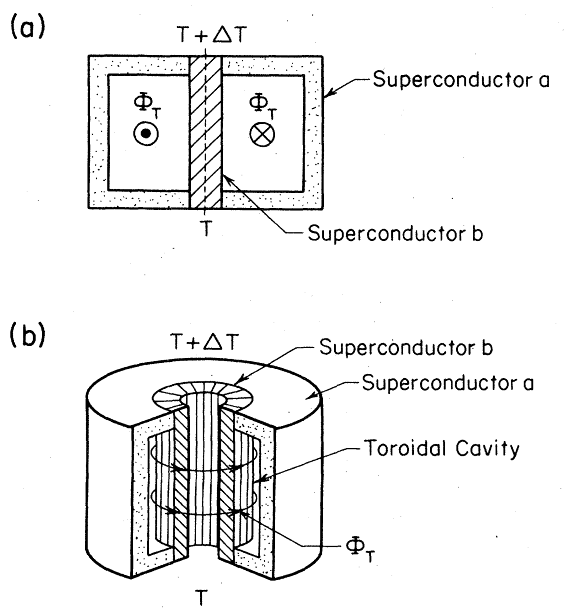

FIG. 4. (a) The thermoelectric flux Φ_T is generated in each side of a double bimetallic loop. (b) Rotation of the loop around the dashed line in (a) generates a toroidal solid. When one face of the toroid is heated, surface currents produce a circulating magnetic flux within the cavity.

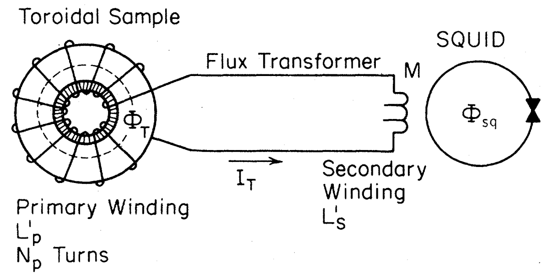

FIG. 5. In the toroidal geometry, the flux Φ_T is coupled into the SQUID magnetometer via a superconducting flux transformer. The flux transfer factor f depends on the mutual inductance M, the screened secondary coil inductance L_s', and the screened inductance L_p' of the N_p-turn primary coil.

now be formed by rotating the double loop about an axis through the center of superconductor b [shown as a dashed line in Fig. 4(a)] to generate a solid of revolution. As shown in Fig. 4(b), superconductor b now becomes a center post while superconductor a forms an outer shell. If a temperature difference is imposed between the top and bottom faces of the toroid, a magnetic flux will circulate within the toroidal cavity. This flux is produced by circulating surface currents which flow on the interior walls of the cavity.

In our experiment, the flux in the cavity is coupled into a SQUID magnetometer by means of a superconducting flux transformer. The primary of the flux transformer is wound around the toroid through a hole in the center superconductor, as illustrated in Fig. 5. The flux circulating in the cavity links the primary winding and induces current in the transformer which is ultimately sensed by the SQUID. An unusual aspect of the experiment is that the magnetic field is shielded by the interior walls of the sample and is confined to the hollow cavity. The vector potential is not shielded by the sample, however, so that the flux transformer is able to detect the existence of the interior flux even in the absence of any magneitc field outside the sample.

2. Flux transformer design

In a conventional flux transformer, a magnetic flux coupled into the primary winding induces current in the transformer whose magnitude is just sufficient to keep the total flux in both windings at its original value, ordinarily zero. In our experiments, the response of the flux transformer is complicated by the superconducting core of the primary winding. As current flows in the transformer, screening currents flow on the outside surface of this core which contribute as additional source of flux to that circulating in the interior of the core. As will be shown below, it is possible to design the flux transformer to take advantage of this additional source of flux, with the result that more flux can actually be coupled into the SQUID than is generated in the cavity. This flux-amplification effect is one of the experimental advantages of the toroidal sample geometry.

The flux transfer efficiency of the circuit of Fig. 5 can be characterized by a flux transfer factor f. This factor is given by

$$f = \delta\Phi_{\rm sq}/\delta\Phi_T \ , \tag{22}$$

where $\delta\Phi_{\rm sq}$ is the incremental flux induced in the SQUID by a thermoelectric flux $\delta\Phi_T$ in the toroidal cavity. In order to calculate f, we note that the total quantized flux $n\Phi_0$ in the transformer is made up of two components, a flux $\Phi_{\rm ext}$ arising from external sources, and an internal flux $\Phi_{\rm int}$ arising from currents circulating in the flux transformer itself. Thus we write

$$n\Phi_0 = \Phi_{\rm ext} + \Phi_{\rm int} = \Phi_{\rm ext} + L^* I_T \ , \tag{23}$$

where I_T is the current in the transformer and L^* is the effective inductance of the flux transformer. If we assume L^* does not change, then $\delta\Phi_{\rm ext} = -L^*\delta I_T$.

The thermoelectric flux $\delta\Phi_T$ links each turn of the primary winding of the flux transformer, so that $\delta\Phi_{\rm ext} = N_p \delta\Phi_T$ where N_p is the number of primary turns. Thus the current change in the transformer can be written as

$$\delta I_T = \frac{N_p}{L^*}\delta\Phi_T \ , \tag{24}$$

and the resultant change of flux in the SQUID as

$$\delta\Phi_{\rm sq} = \frac{N_p M}{L^*}\delta\Phi_T \ . \tag{25}$$

In the above expression, M is the mutual inductance between the SQUID and the secondary winding of the flux transformer.

Next we must calculate the effective transformer inductance L^*. Currents circulating in the transformer generate a magnetic field within the primary winding. This field induces diamagnetic currents on the outer surface of the superconducting sample which screen the field from the interior of the sample. As a consequence of this screening effect, the inductance of the primary winding will be lowered from its unscreened value L_p to an effective screened value L_p'. Similarly, diamagnetic screening currents induced on the interior surfaces of the SQUID will reduce the inductance of the secondary winding of the flux transformer to an effective value L_s'. The total effective transformer inductance L^* is then given by $L^* = L_p' + L_s'$.

Because the screened primary inductance $L_p' \propto N_p^2$, Eq. (25) may be written as

$$\delta\Phi_{\rm sq} \propto \frac{(L_p')^{1/2} M \delta\Phi_s}{L_p' + L_s'} \ . \tag{26}$$

From this expression, it may be seen that the maximum flux is transferred into the SQUID magnetometer when $L_p' = L_s'$. Thus the optimum value of the flux transfer factor is given by

$$f = \frac{N_p}{2}\left[\frac{M}{L_s'}\right] \ . \tag{27}$$

This expression illustrates the need to design the primary winding of the flux transformer with care. One must attempt to make N_p as large as possible, subject to the constraint that L_p' not exceed L_s'. (L_s' is typically about 2 μH.) In practice, one winds the primary windings very tightly so that the screening effect of the superconducting sample reduces the screened inductance associated with each turn to as small a value as possible.

3. *Properties of the toroidal geometry*

As mentioned previously, the toroidal design used in the experiment has improved sensitivity, greater immunity from undesired sources of flux, and greater resistance to penetration depth complications over the loop galvanometer technique used in the experiments of Zavaritskii,[21] Pegrum *et al.*,[22] and Falco.[23] The price paid for these advantages is increased complexity of the experiment and greater difficulty in preparing samples.

Sensitivity. In the galvanometer technique, the superconducting signal coil of a SQUID galvanometer forms one side of a bimetallic loop, as shown in Fig. 6, while the superconducting wire being studied comprises the other side. The SQUID measures the current that produces the thermoelectric flux Φ_T in the loop. The response of the SQUID to the thermoelectric flux Φ_l is given by a flux transfer factor $f_{\rm loop}$, analogous to that previously described for the toroidal geometry. For the loop, the flux transfer factor is

$$f_{\rm loop} = \frac{M}{L_p + L_s'} = \frac{1}{1 + L_p/L_s'}\left[\frac{M}{L_s'}\right] \ , \tag{28}$$

where L_p is the inductance of that part of the loop external to the SQUID signal coil, and L_s' and M are, respectively, that screened inductance of the signal coil and the mutual inductance between the signal coil and the SQUID. Equation (28) shows that $f_{\rm loop}$ has a maximum value of M/L_s' when L_p is made much smaller than L_s'. By comparison with Eq. (27), we see that the toroid exhibits an improved sensitivity of $\frac{1}{2}N_p$ over the loop galvanometer. The sensitivity advantage to be realized in practice is likely to be

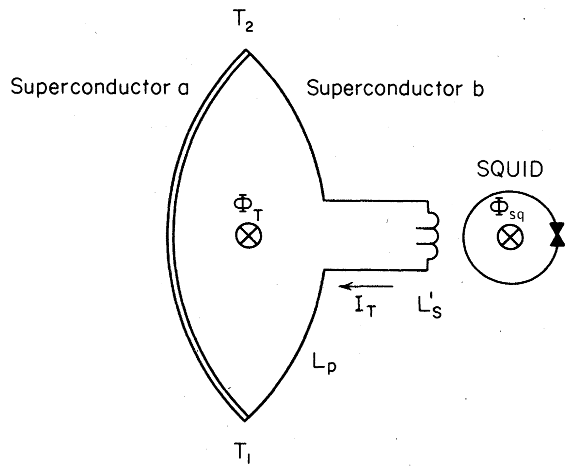

FIG. 6. In the loop galvanometer method, superconductor *a* is the sample while superconductor *b* forms the signal coil of a SQUID galvanometer. The circulating current I_T which produces the flux Φ_T is measured directly by the SQUID.

greater than this factor because of the difficulty in constructing a loop which satisfies the criterion $L_p << L_s'$.

External flux rejection. Extraneous magnetic flux which couples into the SQUID magnetometer cannot only mask the thermoelectric flux but can also be confused for the desired signal. Spurious flux can arise from several sources, primarily electric currents in heaters and thermometers, magnetic materials in the cryostat, surface currents on superconducting flux shields, and thermoelectric currents in normal metals near the sample. In practice, this last source is most troublesome because the field produced by ordinary thermoelectric currents depends on the applied temperature gradient in the same manner as the desired signal. In the loop geometry, unwanted fields are readily coupled into the unscreened inductance of the bimetallic loop where they induce noise currents. In the toroid, the coupling of unwanted fields is greatly reduced, in part because the inherent symmetry of the toroidal geometry cancels external fields to first order, and in part because the superconducting core reduces the effective area of the primary winding.

Penetration depth complications. In a closed superconducting loop the total magnetic flux remains constant, so that any change in the inductance δL of the loop is accompanied by a corresponding change in the current δI in the loop. Clearly $\delta I = \delta(\Phi/L) = -(\Phi/L^2)\delta L$. As the temperature of the loop is varied, changes in the superconducting penetration depth λ change the effective inductance by redistributing the circulating current. This change is approximately given by $\delta L \approx L(C\delta\lambda/A)$, where C and A are the circumference and area of the loop, respectively. The resulting change in current $\delta I \approx (\Phi C/AL)\delta\lambda$ is small, except near T_c where the penetration depth varies rapidly with temperature. Setting $\lambda(t) \approx \frac{1}{2}\lambda_0(1-t)^{-1/2}$, where $t = T/T_c$, we see that a change of loop temperature δt produces a current change of

$$\delta I \approx \Phi \left[\frac{C\lambda_0}{4AL}\right](1-t)^{-3/2}\delta t \quad . \tag{29}$$

In the above expression, δI diverges near the transition as $(1-t)^{-3/2}$, the same temperature dependence observed for the thermoelectric flux Φ_T. It is this similarity which makes the thermoelectric effect difficult to measure unambiguously using the loop geometry. Note also from Eq. (29) that δI scales with the residual flux Φ trapped in the loop. In practice, it is difficult to reduce this trapped flux to the point where δI does not dominate the desired signal; Pegrum and Guénault,[24] in a series of measurements on Nb-Ta loops, found this effect large enough to account for much of their data.

The toroidal geometry is much less susceptible to penetration depth effects than the loop geometry. In the toroid, the currents which produce the flux are on the interior walls of the cavity. The primary of the flux transformer responds to the total flux rather than to these interior currents, so that variations in penetration depth on the inside walls do not change the detected signal. Penetration depth changes on the outside walls of the toroid do contribute to the SQUID response, but this effect is relatively minor. A variation in the penetration depth of the outside walls produces a second order change in the screened inductance L_p' of the flux transformer primary. This change in turn alters the current in the transformer by an amount porportional to the flux trapped inside the flux transformer circuit. The symmetry of the toroidal configuration inherently discriminates against trapped flux, however, so that in practice this contribution to the SQUID signal is not significant.

B. Experimental details

1. Sample construction

The design of the In-Pb toroidal samples used in our experiment is shown in Fig. 7. The toroids were approximately 4 cm long and 7 mm in diameter. The center post of each toroid consisted of a 2-cm by 2-mm diameter 99.999% purity Pb rod through which a 1-mm-diameter hole was drilled lengthwise. A 6-mm-diameter Teflon cylinder was split and placed around the Pb to form the toroidal cavity. Indium disks soldered to each end of the Pb post formed the top and bottom faces of the toroid, while the outer cylindrical surface consisted of 0.25-mm In foil wrapped around

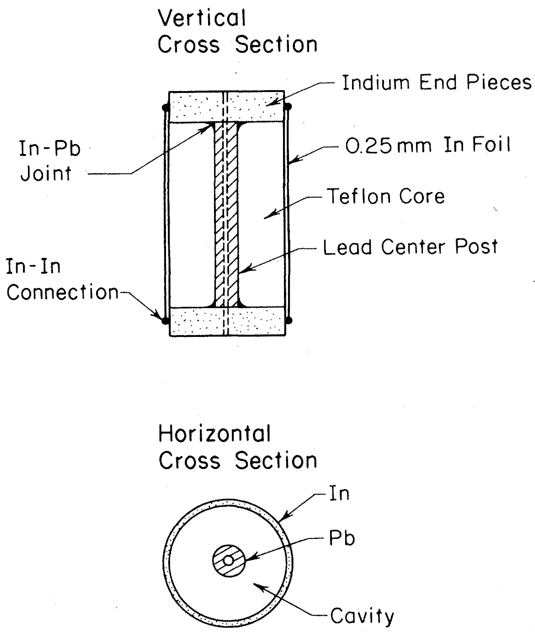

FIG. 7. A toroidal sample consists of a center post of Pb and an outer surface of high-purity In foil. The primary coil of the flux transformer is wound around the sample through a hole in the center.

the assembly and soldered to the edges of the In end pieces.

All of the indium pieces were made from 59-grade polycrystalline In, acid-etched in dilute HNO_3 and annealed at 115 °C for 2 h to obtain a residual resistivity ratio of about 10^4. Care was taken throughout sample construction to minimize contamination of the indium: impurities not only broaden the superconducting transition but also degrade the thermoelectric currents. For the geometry and purity of indium used in our samples, a typical thermal resistance between the toroid faces was $\sim$1 mK/mW.

The flux transformer primary coil consisted of 6–10 turns of 0.003-in. Formvar-insulated Nb wire wound around the toroid through the hole in the center post. To minimize L_p', the turns were tightly wrapped and fastened to the indium surface with G.E. 7031 varnish. The leads to the SQUID were brought off tightly twisted from one end of the sample.

2. *Cryostat design*

The cryostat used in the experiment is illustrated in Fig. 8, while associated instrumentation is shown schematically in Fig. 9. The toroidal sample and SQUID were isolated from the helium bath by an evacuated brass can sealed with an indium O-ring. All electrical leads were brought into the vacuum can through six 10-wire epoxy feed-throughs (Stycast No.

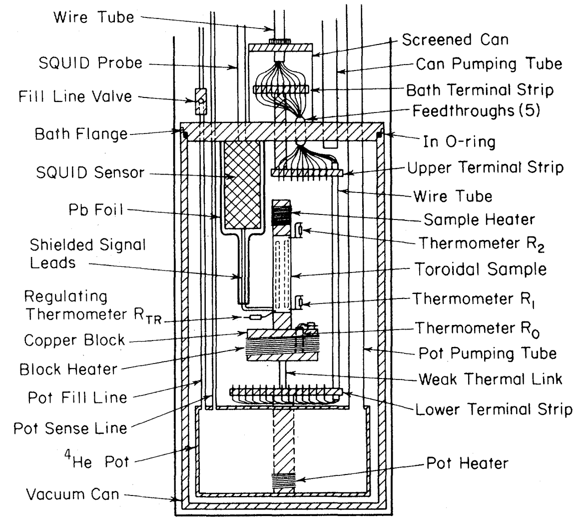

FIG. 8. Lower section of the cryostat used in the experiment.

2850GT) and distributed to terminal strips in the can as shown. Within the vacuum can, a copper ^{4}He pot of volume 340 cm^3 was suspended from the bath plate by three stainless steel tubes which also served as lines for filling, pumping, and pressure sensing. The pot was filled from the bath through a needle valve operated from the top of the Dewar. The tem-

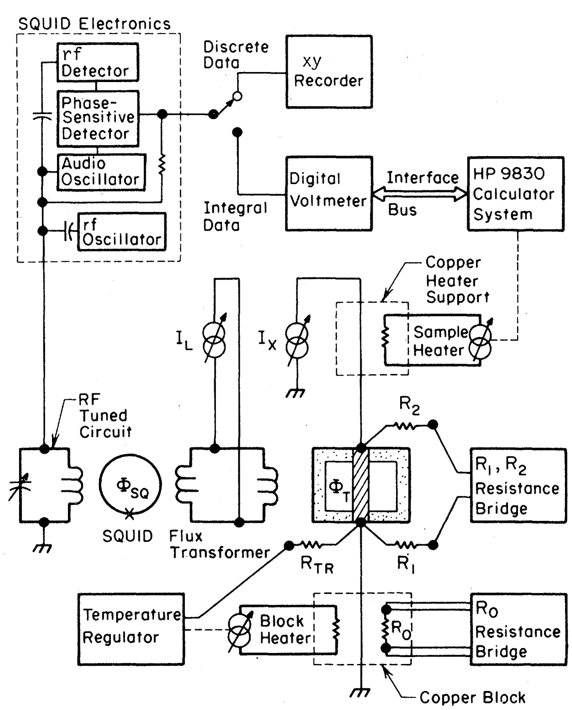

FIG. 9. Schematic drawing of the instrumentation for the thermoelectric-flux experiment.

perature of the pot was controlled between 2.2 K and 4.2 K by a Lakeshore vacuum regulator valve which maintained the vapor pressure to 0.1 Torr; below the λ point, the pot temperature was regulated by a heater located at the bottom of the pot.

The toroidal sample was mounted on a cylindrical copper block supported above the pot by a 0.2 mm wall copper tube. A small copper cylinder attached to the top of the sample served as a former for the sample heater. Both copper pieces were machined from 99.9999% purity polycrystalline copper and oxygen-annealed at 960 °C for two hours to remove traces of magnetic impurities. By this procedure, we reduced the spurious flux from normal thermoelectric currents in the copper to 10^{-3} of the flux observed using ordinary oxygen-free-high-conductivity copper supports. The thermal contacts from the copper pieces to the sample were made with Wood's alloy.

Two heaters, a sample heater and a block heater, were used to control the temperature profile of the sample. Because the sample assembly was thermally isolated, it was possible to establish a uniform temperature by supplying heat only to the block; the sample heater was used to fix a temperature gradient across the toroid. An electronic temperature regulator, used in conjunction with the block heater and a 56 Ω, 0.1 W carbon regulating thermometer at the bottom of the sample, held the lower face of the toroid at a fixed temperature while the temperature gradient was varied. We found that the capability of varying the sample temperature continuously in the absence of a temperature gradient provided a convenient means of checking for spurious penetration depth effects.

The temperatures of the top and bottom faces of the toroid were monitored by matched germanium thermometers R_1 and R_2, located as shown in Fig. 8. A three-wire resistance bridge operated at 138 Hz was used to measure R_1, R_2, and $\Delta R = |R_1 - R_2|$ directly. R_1 and R_2 were calibrated during each run against a germanium standard thermometer R_0 which was thermally anchored to the copper block; a four-terminal active resistance bridge operated at 108 Hz was used to measure R_0.

3. *SQUID magnetometer*

The thermoelectric flux Φ_T was measured with an rf-biased two-hole symmetric Nb SQUID and associated electronics obtained from S.H.E. Corporation. The SQUID sensor was mounted inside the vacuum can and was thermally anchored to the bath flange as shown in Fig. 8. During runs, the bath temperature was regulated at 3.8 K to eliminate drifts in the SQUID critical current. The SQUID was screened from external flux by a Pb-plated brass can and by a layer of 0.004 in. Pb foil.

To minimize rf interference, we conducted the experiment in an RFI/EMI screened room and shielded and filtered all leads to the cryostat. Additionally, a resistive shunt of approximately 2 mΩ was placed across the flux transformer secondary coil to roll off the SQUID high-frequency response at 1 kHz. This value of shunt resistance provided adequate rf rejection without degrading SQUID performance with Johnson noise. The SQUID was operated in a conventional flux-locked mode to produce an output voltage of $10\Phi_0$/V. Typical noise levels were 10^{-3} $\Phi_0 H_z^{-1/2}$ with a dc drift of less than 10^{-4} Φ_0 h^{-1}. Maximum SQUID flux resolution was estimated to be 5×10^{-4} Φ_0.

Because of the extreme sensitivity of the experiment, we found it necessary to take the following precautions to minimize stray magnetic fields: (1) All current-carrying wires were run in twisted pairs shielded by superconducting tubes; (2) the block and sample heaters were wound noninductively and enclosed in Pb foil; (3) the formers on which the heaters were wound were made of oxygen annealed 69-grade copper (to minimize normal-state thermoelectric currents in the formers); (4) the sample was screened from external fields by lead plating the interior of the vacuum can and by enclosing the entire probe in a Pb foil bag; (5) the Dewar was surrounded by a μ-metal shield to reduce the static flux trapped in the Pb shields and in the flux transformer circuit. The residual field within the shield was less than 10^{-3} G at room temperature.

4. *Data acquisition*

In the experiment, two procedures were used to measure the thermoelectric coefficient $\Omega(T)$. At temperatures well below T_c, $\Omega(T)$ was obtained by monitoring the SQUID output on an x-y recorder as a function of the temperature difference across the sample. Then, for small ΔT, $\Omega(T)$ was given simply by $\Omega(T)\approx\Delta\Phi_T/\Delta T$.

Very near T_c, however, $\Omega(T)$ diverged rapidly, making it impractical to obtain data in the above manner. In this range, $\Omega(T)$ was measured by an "integral" method. With the bottom face of the sample held at a fixed temperature $T_1 < T_c$, the top face was heated by gradually increasing sample heat. During this procedure, the flux $\Delta\Phi_T$ was recorded as a function of the temperature of the hot end of the sample. $\Delta\Phi_T$ is given by

$$\Delta\Phi_T(T,T_1)=\int_{T_1}^{T}\Omega(T')\,dT' \ , \tag{30}$$

so that $\Omega(T)$ may be obtained by differentiation; i.e.,

$$\Omega(T)=\frac{d\Phi_T(T,T_1)}{dT} \ . \tag{31}$$

In practice, the sample heat was incremented in approximately 50 μW steps, and the SQUID output and ΔT at each level were recorded by a digital acquisition system.

IV. EXPERIMENTAL RESULTS

A. Properties of bulk indium

Indium is a trivalent metal whose band structure is similar to that of most free-electron-like metals. The Fermi surface of In resembles closely that of Al, a metal whose Fermi parameters and transport coefficients have been extensively studied. Unlike Al, however, the thermoelectric power $S(T)$ of In does not have the negative linear temperature dependence of a free-electron conductor. Instead, the thermoelectric power of In fluctuates widely with temperature, undergoing several reversals in sign at low temperatures. Although there is no comprehensive low-temperature study of the thermoelectric power of In, it appears that there is a positive peak in $S(T)$ at about 20 K, a sign reversal at about 10 K, and another sign reversal near the superconducting transition temperature.[29] The precise temperatures at which these sign reversals occur vary from sample to sample. As will be discussed below, we have found the thermoelectric power of normal-state In just above T_c to vary widely among different samples; in most of our samples $S(T_c)$ was positive, although in two samples it was negative.

In order to facilitate comparison with the thermoelectric properties of superconducting In, we have measured the normal-state thermoelectric coefficient $L_T(T)$ in addition to the thermoelectric power $S(T)$. As discussed in Sec. II, $L_T(T)$ is a measure of the electric current $\vec{J}$ resulting from a temperature gradient $\vec{\nabla} T$:

$$L_T(T) = (J/\vec{\nabla} T)_{E'=0} \; . \tag{32}$$

It is possible to obtain $L_T(T)$ by making simultaneous measurements of $S(T)$ and the resistivity $\rho(T)$ and by invoking the identity $L_T(T) = S(T)/\rho(T)$. In Fig. 10, we show the temperature dependence of $S(T)$ and $L_T(T)$ for the 59-grade pure In which was the starting material for all of our samples. For this material, the thermoelectric power $S(T)$ was positive at T_c with a value of about 10^{-7} V/K—typical of a pure metal at low temperatures. As expected, $S(T)$ vanished below T_c; however, were one to suppress the superconductivity by applying a weak magnetic field, it is reasonable to assume that $S(T)$ would reach a positive maximum at some temperature below T_c and fall to zero at zero temperature. [Thermodynamic considerations require $S(T)=0$ at $T=0$.] The temperature dependence of $L_T(T)$ resembles that of $S(T)$ in that it exhibits a rapid in-

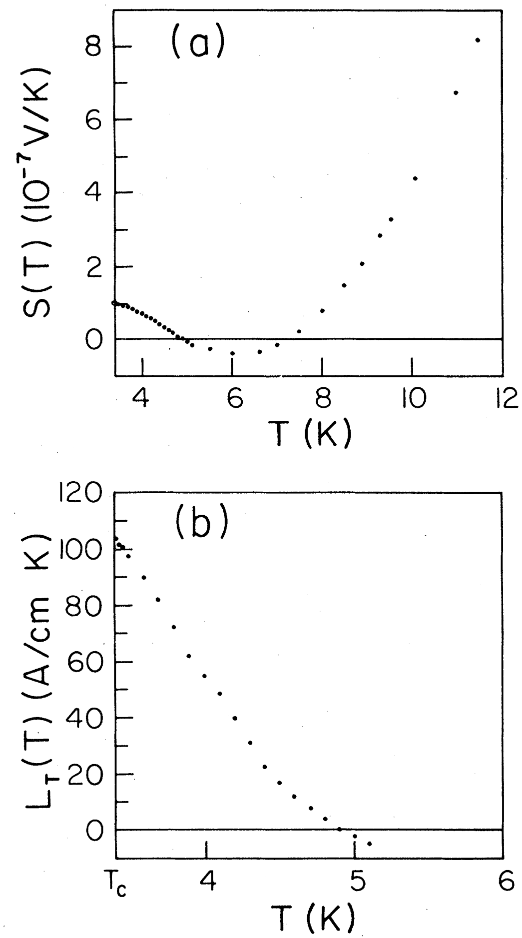

FIG. 10. (a) The temperature dependence of the thermoelectric power $S(T)$ of the pure indium starting material used in the toroidal samples, illustrating the sign reversals in $S(T)$ at low temperatures. (b) The temperature dependence of the normal-state thermoelectric coefficient $L_T(T)$ for the pure indium.

TABLE I. Sample properties.

Sample No.	RRR	$\kappa(T_c)$ (W/cm K)	$L_T(T_c)$ (A/cm K)	Ω_0 (Φ_0/K)
T-1	6390	43.2	19.7	0.19
T-2	8520	46.5	−213.4	−6.64
T-3	8480	59.2	100.0	1.45
T-4	8550	40.1	98.2	0.62
T-5	8700	36.8	52.3	0.72
T-6	8710	12.3	25.8	0.23
T-7	292	2.3	−11.9	−1.58

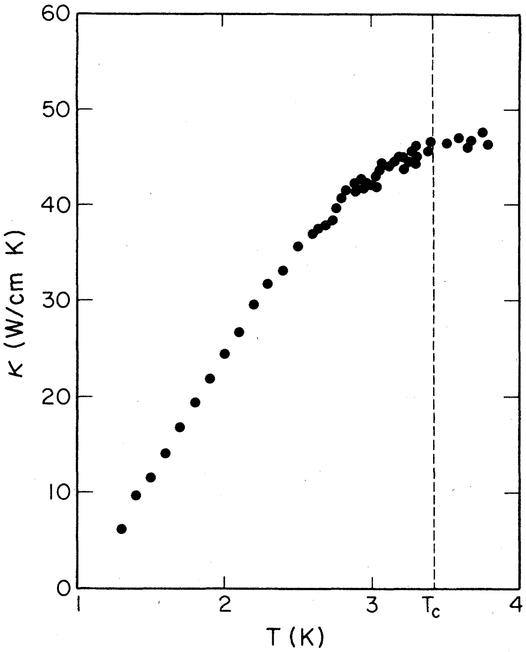

FIG. 11. The temperature dependence of the thermal conductivity $\kappa(T)$ of pure bulk indium in the superconducting state.

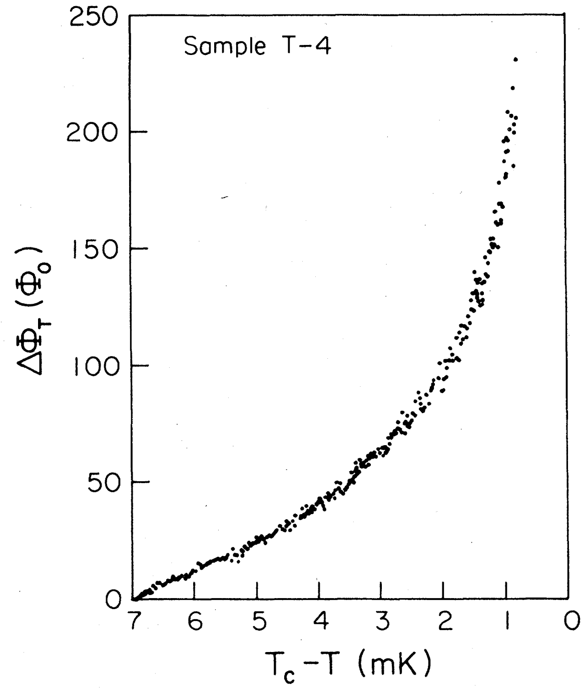

FIG. 12. The temperature dependence of the flux generated in toroidal In-Pb sample T-4; the data were obtained by fixing the one face of the toroid at $T_c - T = 7$ mK and heating the other face in 50 μK steps toward T_c.

crease as the temperature is lowered toward T_c. In Table I, we show the measured value of $L_T(T_c)$ for the In constituent of all our toroidal samples.

Table I also gives the residual resistivity ratio (RRR) and the thermal conductivity $\kappa(T_c)$ of In for all samples. As shown in Fig. 11, $\kappa(T)$ in superconducting In decreases smoothly to zero, reflecting the decrease in the quasiparticle population as the temperature is lowered below T_c.

B. Thermoelectric effect in superconducting indium

In Fig. 12, we show the temperature dependence of the flux $\Delta\Phi_T$ generated in a toroidal In-Pb specimen (sample T-4) which results from the application of a temperature difference across the faces of the toroid. For these data, which are representative of the data obtained for all specimens, the bottom face of the toroid was fixed at $T = T_c - 7.0$ mK, while the upper face of the toroid was heated in 50 μK steps toward T_c. The value of T_c could be obtained to within 0.2 mK by observing the decrease below T_c in the sensitivity of the SQUID detector to external magnetic fields.[30] It was not possible for us to obtain thermoelectricity data closer to T_c than about 0.5 mK because the rapid divergence of $\Delta\Phi_T$ near T_c caused the SQUID to unlock from the flux-locked mode. As discussed in Sec. III, the thermoelectric coefficient $\Omega(T)$ was obtained by differentiating curves similar to Fig. 12 for each of our seven torodial samples.

The results for all of our toroidal samples are summarized in Fig. 13, which shows the temperature dependence of the thermoelectric coefficient $\Omega(T)$ in units of Φ_0/K; $\Omega(T)$ was negative for samples T-2 and T-7, so the figure plots $-\Omega(T)$ for those samples. For each specimen, $\Omega(T)$ diverged as T_c was approached from below. To within the resolution of the data, the temperature dependence of $\Omega(T)$ could be expressed as

$$\Omega(T) = \Omega_0(1 - T/T_c)^{-3/2} \ , \qquad (33)$$

where Ω_0 is a constant which varied from sample to sample by about a factor of 40: $0.19\Phi_0/\mathrm{K} < |\Omega_0| < 6.6\Phi_0/\mathrm{K}$.

There did not appear to be any obvious correlation of the magnitude of Ω_0 with the RRR of the samples. For example, samples T-3 and T-7 had essentially the same magnitude of Ω_0 although their RRR differed by a factor of 30. On the other hand, there did appear to be a direct correlation of Ω_0 with L_T, the normal-state thermoelectric coefficient. This relationship is shown in Fig. 14, which plots Ω_0 for each of the seven samples as a function of L_T. The data of Fig. 14 may by summarized by the following

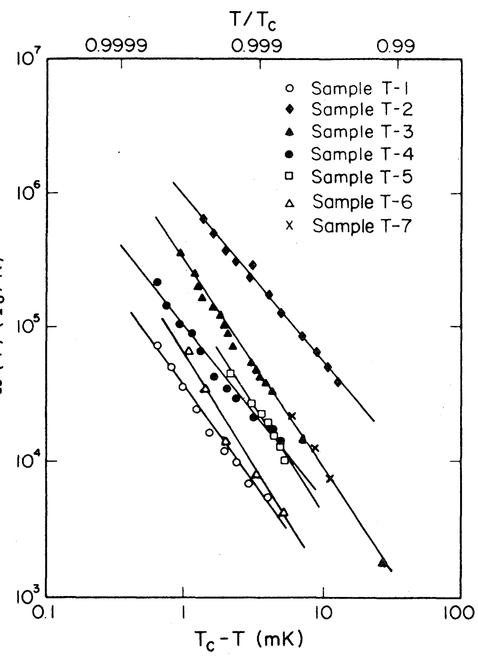

FIG. 13. The temperature dependence of the thermoelectric coefficient $\Omega(T)$ of superconducting indium for seven In-Pb toroidal samples. To within the resolution of the data, all samples exhibited a $(1-T/T_c)^{-3/2}$ divergence.

empirical realtion:

$$\Omega_0 = \alpha L_T(T_c) \quad , \tag{34}$$

where $\alpha \approx 10^{-2}\Phi_0$ cm/A. In showing this correlation, it is fortunate that the sign of the thermoelectric coefficients of two of the samples was negative.

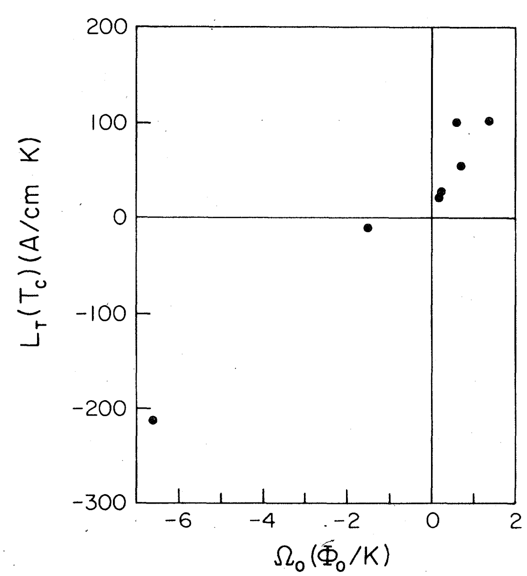

FIG. 14. Relationship between the normal-state thermoelectric coefficient $L_T(T_c)$ and the superconducting coefficient Ω_0 for seven toroidal In-Pb samples.

C. Tests for spurious effects

In order to verify that the flux detected by the SQUID magnetometer was actually associated with a thermoelectric flux in the cavity of the toroidal samples, we performed a number of consistency checks. First, we fabricated a dummy sample which had exactly the same construction as our regular samples except that both halves of the toriod were made of indium. In such a sample, one would not expect to see any temperature-dependent flux in the superconducting state. The measurements made on this dummy sample are shown in Fig. 15. These data were obtained by fixing the bottom face of the toroid about 3 mK below T_c and gradually heating the top face up through T_c. As shown in the figure, there was no detectable flux induced into the SQUID until T_c was reached. At temperatures above T_c, the SQUID recorded a flux which increased with the temperature difference across the sample. This normal-state flux is a result of circulating thermoelectric currents induced in the normal indium by the temperature difference. These currents would vanish in a perfectly homogeneous specimen of indium; however, because of slight differences in the RRR of the two halves of the indium sample, the normal currents do not cancel completely and are easily detected by the SQUID.

Figure 16 shows the results of tests intended to see whether our data could result from temperature-

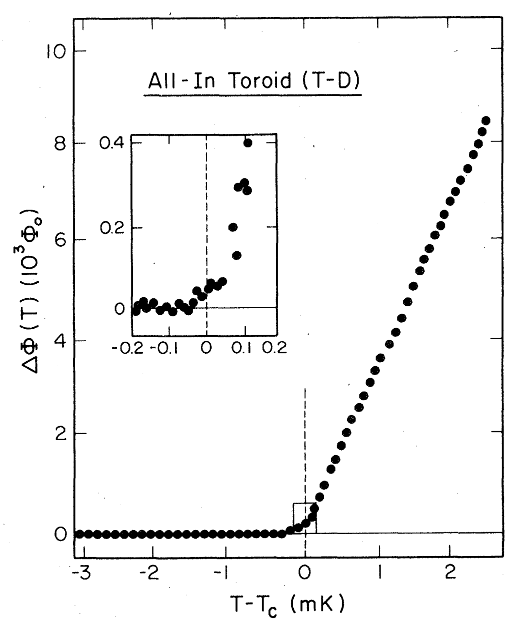

FIG. 15. The temperature dependence of the flux generated in a dummy In-In toroidal sample; the data were obtained by fixing one face of the toroid at $T_c - T = 3$ mK and heating the other face up through the superconducting transition.

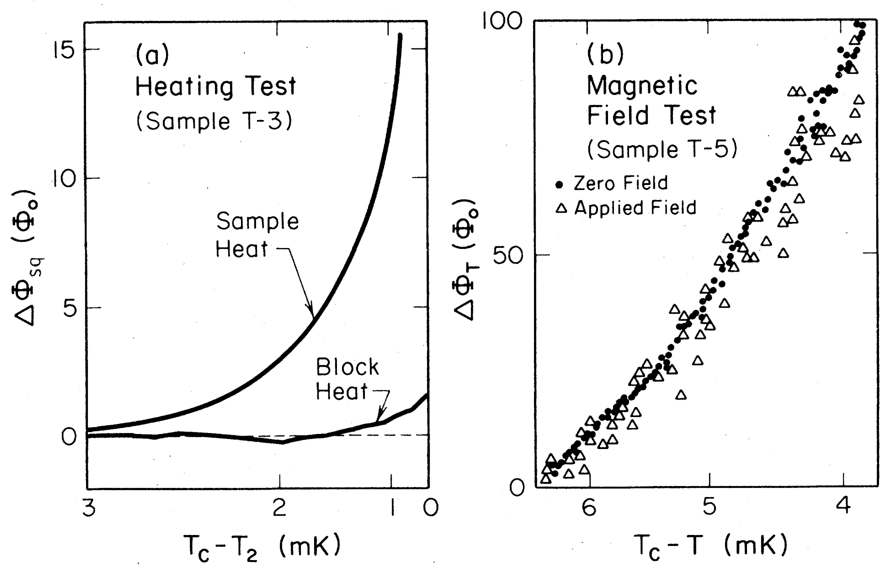

FIG. 16. (a) x-y recorder tracings comparing the SQUID flux generated by heating sample T-3 uniformly and by applying a temperature gradient across the sample. (b) Thermoelectric flux generated in sample T-5 taken before and after application of an external magnetic field.

dependent changes in the superconducting penetration depth of the indium. Because such changes can in principle produce a flux which has the same divergent temperature dependence observed in our measurements (see Sec. III), we took careful steps to ensure that our observed effects did not have this spurious origin. According to Eq. (29), a penetration-depth-induced flux would be expected to scale with the current circulating in the flux transformer (either a persistent current, or a screening current arising from an external source of magnetic field). In addition, a flux arising from changes in the penetration depth would increase with the average temperature of the sample, rather than with the temperature difference across the sample. Figure 16(a) compares the flux produced in the SQUID when sample T-3 was heated uniformly to the flux produced when a temperature difference was applied across the sample. In the first case, the entire sample was heated by about 2 mK, while in the second case the bottom of the toroid was held at a fixed temperature and the top of the toroid was heated by 2 mK. It is clear from the figure that a uniform heating of the sample does not produce any appreciable flux.

Figure 16(b) compares the temperature-dependent flux recorded by the SQUID detector for sample T-5 before and after an external magnetic field was allowed to link the flux transformer. The external field was estimated to induce a flux of about $10^4\ \Phi_0$ into the flux transformer. Although the screening currents resulting from this large external flux caused some degradation of the signal-to-noise ratio of the thermoelectric flux (because of vibration), it is obvious that no significant change in the thermoelectric flux could be observed. On the basis of these tests, therefore, we believe it is possible to conclude that complications arising from the penetration depth are not responsible for the effect we have observed.

V. DISCUSSION

Our measurements of a thermoelectrically induced flux in seven torodial Pb-In specimens have confirmed qualitatively the model for thermoelectricity discussed in Sec. II. In particular, we have shown that the thermoelectric flux is induced by a temperature gradient, that it scales with the normal thermoelectric coefficient L_T, diverges near T_c, and vanishes for a monometallic specimen. In analyzing our results, we have characterized this flux by a coefficient $\Omega(T)$ which was shown in Sec. II to be given by

$$\Omega(T)=\frac{mc}{e^2}\frac{L_T(T)}{n_s(T)} \quad . \tag{35}$$

The divergence in $\Omega(T)$ as $T\to T_c$ is to be expected from the factor of n_s in the denominator of Eq. (35). It is possible to express n_s in terms of the superconducting order parameter $\Delta(T)$:

$$n_s=n_0\frac{\Delta^2(T)}{\Delta^2(0)} \quad . \tag{36}$$

Using the BCS expression for $\Delta(T)$, n_s is found to depend only on the reduced temperature $t=T/T_c$ and to vary near $t=1$ as $3.0n_0(1-t)$. Thus we expect $\Omega(T)$ to be given near the transition temperature by

$$\Omega(t)=\frac{mc}{3.0\,n_0e^2}\frac{L_T(t)}{(1-t)} \quad . \tag{37}$$

Combining this expression with our experimental results, summarized by Eqs. (33) and (34), we obtain an empirical expression for the superconducting transport coefficient L_T of indium:

$$L_{(T)}=2.0\times 10^3 L_T(T_c)\left(1-\frac{T}{T_c}\right)^{-1/2} \quad . \tag{38}$$

Equation (38) may be compared directly with calculations of the thermoelectric coefficient obtained by solving the microscopic kinetic equation for the nonequilibrium quasiparticle distribution. Because of the sensitivity of the thermoelectric coefficient to scattering details, such a microscopic calculation is difficult, even for normal metals. In superconductors, the problem is complicated by the existence of the energy gap, the superfluid counterflow, and by relaxation processes which occur only in the superconducting state.

The only existing calculation of L_T is that of Gal'perin *et al.*,[9] which ignores the complications of the superfluid condensate and assumes that scattering of quasiparticles is the same as for normal electrons. Their calculations produces the result that, for the temperature regime investigated in our experiments, $L_T \approx L_T(T_c)$, i.e., that there should be no discontinuity in the thermoelectric transport coefficient at the superconducting transition. It is clear that there is gross disagreement between this prediction and the results of our experiment, not only in the temperature dependence of L_T but also in its overall magnitude. In essence, the observed thermoelectric effect is about five orders of magnitude larger than one would expect by assuming a direct parallel between normal-state and superconducting-state thermoelectricity.

There are several possibilities which could account for this discrepancy. First, it may be necessary to construct a theory for thermoelectricity in superconductors which accounts for transport processes unique to the superconducting state, specifically the superfluid counterflow current and the relaxation of excess quasiparticle charge into the superfluid condensate. The relevance of the counterflow current becomes evident when one realizes that the velocity of the flow $\vec{v}_s$ becomes very large near T_c. The effect of this superfluid motion is to introduce an anisotropy $h\vec{k}\cdot\vec{v}_s$ into the excitation spectrum of the quasiparticles and to reduce the chemical potential of the superconduting condensate by the Bernoulli term $\frac{1}{2}mv_s^2$. The influence of these terms on the transport coefficient L_T is not completely clear, although it is believed that they introduce additional asymmetries into the quasiparticle distribution function. In our opinion, however, it is unlikely that these corrections to the distribution function will predict thermoelectric currents which are linear in $\vec{\nabla}T$; all of our data suggest that the thermoelectric flux is linear in $\vec{\nabla}T$.

A second possible explanation is that there are sources of thermoelectrically-induced flux which are not included in Eq. (21). Our model considers the flux induced within the toroidal cavity of our samples by currents which flow on the inside walls of the cavity. There may also be thermoelectric currents on the outside surface of the samples which produce a flux which would be detected by the flux transformer in our experiment. It is not obvious that such currents actually exist; if they do, one could in principle explain them by solving a boundary-value problem for the vector potential $\vec{A}$ subject to certain assumptions about the manner in which the normal quasiparticle current was clamped at the surface.

Finally, there is the unfortunate possibility that our data are not associated with thermoelectricity in superconductors at all but result from some spurious effect. We have tried to take every precaution to minimize this possiblity, but we cannot eliminate it entirely until our results are corroborated by other experiments.

ACKNOWLEDGMENTS

The authors are grateful for helpful discussions with W. E. Lawrence, B. R. Patton, A. Schmid, P. L. Taylor, and J. R. Waldram. The authors have also profited by a critical reading of the manuscript by Y. A. Ono. This research was supported by the NSF, Grant No. DMR 78-09428.

---

*Present address: Dept. of Phys. Univ. of Calif. at Berkeley, Berkeley, Calif. 94720.

[1]G. M. Eliashberg, Zh. Eksp. Teor. Fiz. 61, 1254 (1971) [Sov. Phys. JETP 34, 668 (1972)].

[2]A. Schmid and G. Schön, J. Low Temp. Phys. 20, 207 (1975).

[3]C. Pethick and H. Smith, J. Phys. (Paris) 39, C6-488 (1978).

[4]S. B. Kaplan, C. C. Chi, D. N. Langenberg, J. J. Chang, S. Jafarey, and D. J. Scalapino, Phys. Rev. B 14, 4854 (1976).

[5]W. E. Lawrence and A. B. Meador, Phys. Rev. B 18, 1154 (1978).

[6]M. Tinkham, Phys. Rev. B 6, 1747 (1972).

[7]A. A. J. Matsinger, R. de Bruyn Ouboter, and H. van Beeken, Physica (Utrecht) B 93, 63 (1978).

[8]J. C. Garland and D. J. van Harlingen, Phys. Lett. A 47, 423 (1974).
[9]Yu. M. Gal'perin, V. L. Gurevich, and V. I. Kozub, Zh. Eksp. Teor. Fiz. 66, 1387 (1974) [Sov. Phys. JETP 39, 680 (1975)].
[10]V. L. Ginzburg, Zh. Eksp. Teor. Fiz. 14, 177 (1944) [Sov. Phys. JETP 8, 148 (1944)].
[11]V. Z. Kresin and V. A. Litovchenkȯ, Pis'ma Zh. Eksp. Teor. Fiz. 21, 42 (1975) [JETP Lett. 21, 19 (1975)].
[12]V. L. Ginzburg and G. F. Zharkov, Pis'ma Zh. Eksp. Teor. Fiz. 20, 658 (1974) [JETP Lett. 20, 302 (1974)].
[13]L. Z. Kon, Zh. Eksp. Teor. Fiz. 70 286 (1976) [Sov. Phys. JETP 43, 149 (1976)].
[14]A. G. Aronov, Zh. Eksp. Teor. Fiz. 67, 178 (1974) [Sov. Phys. JETP 40, 90 (1975)].
[15]V. I. Kozub, Zh. Eksp. Teor. Fiz. 74, 344 (1978) [Sov. Phys. JETP 47, 178 (1978)].
[16]D. F. Heidel and J. C. Garland, J. Phys. (Paris) 39, C6-492 (1978).
[17]S. N. Artemenko and A. F. Volkov, Zh. Eksp. Teor. Fiz. 70, 1051 (1976) [Sov. Phys. JETP 43, 548 (1976)].
[18]C. Pethick and H. Smith (unpublished).
[19]A. Schmid and G. Schön (unpublished).
[20]R. A. Sacks, J. Low Temp. Phys. 34, 393 (1979).
[21]N. V. Zavaritskii, Pis'ma Zh. Eksp. Teor. Fiz. 19, 205 (1974) [JETP Lett. 19, 126 (1974)].
[22]C. M. Pegrum, A. M. Guénault, and G. R. Pickett, in *Low Temperature Physics-LT14,* edited by M. Krusius and M. Vuario (North-Holland, Amsterdam, 1975), Vol. II, p. 513.
[23]C. M. Falco, Solid State Commun. 19, 623 (1976).
[24]C. M. Pegrum and A. M. Guénault, Phys. Lett. A 59, 393 (1976).
[25]D. J. Van Harlingen and J. C. Garland, Solid State Commun. 25, 419 (1978).
[26]A. de Waele, R. de Bruyn Ouboter, and P. B. Pipes, Physica (Utrecht) 65, 587 (1973).
[27]S. N. Artemenko and A. F. Volkov, Pis'ma Zh. Eksp. Teor. Fiz. 70, 1051 (1976) [JETP Lett. 70, 548 (1976)].
[28]J. R. Waldram, Proc. R. Soc. London, Ser. A 345, 231 (1975).
[29]A. D. Caplin, C. K. Chiang, J. Tracy, and P. A. Schroeder, Phys. Status Solidi A 26, 497 (1974).
[30]This decrease in sensitivity actually denotes the low-temperature edge of the transition, which may be several mK wide in pure indium.